PHYSICAL REVIEW D **86,** 054501 (2012)

Chromoelectric flux tubes and coherence length in QCD

Paolo Cea*
Dipartimento di Fisica dell'Università di Bari, I-70126 Bari, Italy and INFN-Sezione di Bari, I-70126 Bari, Italy

Leonardo Cosmai†
INFN-Sezione di Bari, I-70126 Bari, Italy

Alessandro Papa‡
Dipartimento di Fisica dell'Università della Calabria, I-87036 Arcavacata di Rende, Cosenza, Italy and INFN-Gruppo collegato di Cosenza, I-87036 Arcavacata di Rende, Cosenza, Italy
(Received 11 July 2012; published 5 September 2012)

The transverse profile of the chromoelectric flux tubes in SU(2) and SU(3) pure gauge theories is analyzed by a simple variational ansatz using a strict analogy with ordinary superconductivity. Our method allows to extract the penetration length and the coherence length of the flux tube.

DOI: 10.1103/PhysRevD.86.054501 PACS numbers: 11.15.Ha, 12.38.Aw

I. INTRODUCTION

The presence of chromoelectric flux tubes in QCD vacuum is a clear signal of color confinement [1,2]. Monte Carlo simulations of lattice QCD can produce a sample of vacuum configurations, thus allowing a thorough nonperturbative study of tubelike structures that emerge by analyzing the chromoelectric fields between static quarks [3–19]. A direct consequence of the tubelike structure of the chromoelectric fields between static quarks is the linear potential and hence the color confinement.

A striking physical analogy exists between the QCD vacuum and an electric superconductor. As conjectured a long time ago by 't Hooft [20] and Mandelstam [21], the vacuum of QCD could be modeled as a coherent state of color magnetic monopoles, which is well known as a dual superconductor [22]. In the dual superconductor model of QCD vacuum, the condensation of color magnetic monopoles is analogous to the formation of Cooper pairs in the BCS theory of superconductivity. Even if the dynamical formation of color magnetic monopoles is not explained by the 't Hooft construction, there are a lot of lattice evidences [23–31] for the color magnetic condensation in QCD vacuum. It should be recognized [32] that the color magnetic monopole condensation in the confinement mode of QCD could be a consequence rather than the origin of the mechanism of color confinement, which actually could be originated from additional dynamical causes. Notwithstanding the dual superconductivity picture of the QCD vacuum remains at least a very useful phenomenological frame to interpret the vacuum dynamics.

In the usual electric superconductivity tubelike structures arise [33] as a solution of the Ginzburg-Landau equations. Similar solutions were found by Nielsen and Olesen [34] in the case of the Abelian Higgs model, where they showed that a vortex solution exists independently of the type I or type II superconductor behavior of the vacuum. In previous studies [12–16,35] performed by some of the present authors, color flux tubes made up of chromoelectric field directed along the line joining a static quark-antiquark pair has been investigated, in the cases of SU(2) and SU(3).

In the present work we would like to push forward the analogy with electric superconductivity and exploit some results [36] in the superconductivity to further extract information from flux tube configurations in SU(2) and SU(3) vacuum. The method and the numerical results for both SU(2) and SU(3) are reported in Sec. II. In Sec. III we check the scaling of the penetration and coherence lengths for both SU(2) and SU(3), and compare with previous studies. In Sec. IV we critically discuss the contribution of the longitudinal chromoelectric field to the string tension. Finally, in Sec. V we summarize our results and present our conclusions.

II. CHROMOELECTRIC FLUX TUBES ON THE LATTICE

To explore on the lattice the field configurations produced by a static quark-antiquark pair we exploit the following connected correlation function [7,8,37,38]

$$\rho_W = \frac{\langle \mathrm{tr}(WLU_PL^\dagger)\rangle}{\langle \mathrm{tr}(W)\rangle} - \frac{1}{N}\frac{\langle \mathrm{tr}(U_P)\mathrm{tr}(W)\rangle}{\langle \mathrm{tr}(W)\rangle}, \qquad (1)$$

where $U_P = U_{\mu\nu}(x)$ is the plaquette in the (μ, ν) plane, connected to the Wilson loop W by a Schwinger line L, N is the number of colors (see Fig. 1 in Refs. [16,35]). The correlation function defined in Eq. (1) measures the field strength. Indeed, in the naive continuum limit [8]

$$\rho_W \overset{a\to 0}{\to} a^2 g[\langle F_{\mu\nu}\rangle_{q\bar{q}} - \langle F_{\mu\nu}\rangle_0], \qquad (2)$$

*paolo.cea@ba.infn.it
†leonardo.cosmai@ba.infn.it
‡papa@cs.infn.it

where $\langle \quad \rangle_{q\bar{q}}$ denotes the average in the presence of a static $q\bar{q}$ pair and $\langle \quad \rangle_0$ is the vacuum average. According to Eq. (2), we define the color field strength tensor as

$$F_{\mu\nu}(x) = \sqrt{\frac{\beta}{2N}}\rho_W(x). \tag{3}$$

By varying the distance and the orientation of the plaquette U_P with respect to the Wilson loop W, one can probe the color field distribution of the flux tube. In particular, the case of plaquette parallel to the Wilson loop corresponds to the component of the chromoelectric field longitudinal to the axis defined by the static quarks. In previous studies, the formation of chromoelectric flux tubes was investigated in SU(2) lattice gauge theory [10,12–16] and in SU(3) lattice gauge theory [35] by exploiting the connected correlation function Eq. (1). It was found that the flux tube is almost completely formed by the longitudinal chromoelectric field, E_l, which is constant along the flux axis and decreases rapidly in the transverse direction x_t. By interpreting the formation of chromoelectric flux tubes as dual Meissner effect in the context of the dual superconductor model of confinement, the proposal was advanced [10,12–16] to fit the transverse shape of the longitudinal chromoelectric field according to

$$E_l(x_t) = \frac{\phi}{2\pi}\mu^2 K_0(\mu x_t), \qquad x_t > 0. \tag{4}$$

Here, K_0 is the modified Bessel function of order zero, ϕ is the external flux, and $\lambda = 1/\mu$ is the London penetration length. Equation (4) is valid in the region $x_t \gg \xi$, ξ being the coherence length which measures the coherence of the magnetic monopole condensate (the dual version of the Cooper condensate). In fact, we expect that Eq. (4) gives an adequate description of the transverse structure of the flux tube if $\lambda \gg \xi$. This means that Eq. (4) should be valid for $\kappa \gg 1$ (type II superconductor), where κ is the Ginzburg-Landau parameter,

$$\kappa = \frac{\lambda}{\xi}. \tag{5}$$

However, several numerical studies [9,39–48] in both SU(2) and SU(3) lattice gauge theories indicated that the vacuum behaves like an effective dual superconductor which belongs to the borderline between a type I and type II superconductor with $\kappa \sim 1$. Thus, we see that Eq. (4) is no longer adequate to account for the transverse structure of the longitudinal chromoelectric field. Remarkably, it turns out that we may reanalyze our lattice data for chromoelectric flux tubes by exploiting the results presented in Ref. [36] where, from the assumption of a simple variational model for the magnitude of the normalized order parameter of an isolated vortex, a simple analytic expression is derived for the magnetic field and supercurrent density that solve Ampere's law and the Ginzburg-Landau equation. In particular, the transverse distribution of the magnetic filed reduces to the London model results outside the vortex core, but has the added advantage of yielding realistic values in the vortex core vicinity. Accordingly, from Eq. (4) of Ref. [36] we derive

$$E_l(x_t) = \frac{\phi}{2\pi}\frac{1}{\lambda\xi_v}\frac{K_0(R/\lambda)}{K_1(\xi_v/\lambda)}, \tag{6}$$

with

$$R = \sqrt{x_t^2 + \xi_v^2}, \tag{7}$$

where ξ_v is a variational core radius parameter found to be [36] of the order of ξ. Equation (6) can be written as

$$E_l(x_t) = \frac{\phi}{2\pi}\frac{\mu^2}{\alpha}\frac{K_0[(\mu^2 x_t^2 + \alpha^2)^{1/2}]}{K_1[\alpha]}, \tag{8}$$

with

$$\mu = \frac{1}{\lambda}, \qquad \frac{1}{\alpha} = \frac{\lambda}{\xi_v}. \tag{9}$$

By fitting Eq. (8) to our flux tubes data, we may obtain both the penetration length λ and the ratio of the penetration length to the variational core radius parameter λ/ξ_v. It is worthwhile to recall that, by means of Eq. (8), we can extend our fit up to $x_t = 0$. Moreover by using Eq. (16) of Ref. [36], we may also obtain the Ginzburg-Landau κ parameter,

$$\kappa = \frac{\sqrt{2}}{\alpha}[1 - K_0^2(\alpha)/K_1^2(\alpha)]^{1/2}, \tag{10}$$

where K_1 is the modified Bessel function of order 1. The coherence length ξ is obtained from Eqs. (5) and (10). Our data for chromoelectric fields between static quark-antiquark sources have been obtained through the connected correlation function Eq. (1). In order to reduce the quantum fluctuations we adopted the controlled cooling algorithm. It is known [49] that by cooling in a smooth way equilibrium configurations, quantum fluctuations are reduced by a few orders of magnitude, while the string tension survives and shows a plateau. We shall show below that the penetration length behaves in a similar way. The details of the cooling procedure are described in Ref. [16] for the case of SU(2). Here we adapted the procedure to the case of SU(3), by applying successively this algorithm to various SU(2) subgroups. The control parameter δ was fixed at the value 0.0354, as in Ref. [16]. As described in Ref. [35], in the construction of the lattice operator given in Eq. (1) we have considered also noninteger distances to check the restoration of the rotational symmetry on our lattices.

A. SU(2) data

We analyzed our lattice SU(2) data collected for three different values of β, namely $\beta = 2.52$, 2.55, 2.6 (for further details we refer to Ref. [35]). Indeed, we find that

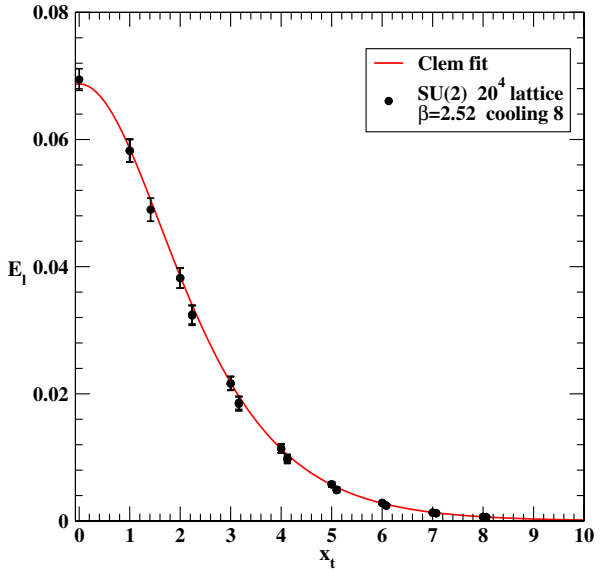

FIG. 1 (color online). SU(2): E_l versus x_t for $\beta = 2.52$ after 8 cooling steps.

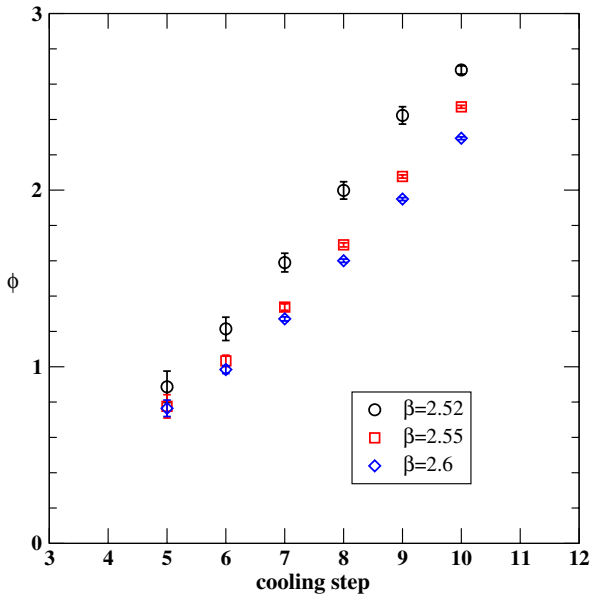

FIG. 2 (color online). SU(2): ϕ versus cooling.

Eq. (8) is able to reproduce the transverse distribution of the longitudinal chromoelectric field in the whole region $x_t \geq 0$. An example of the of effectiveness of Eq. (8) to fit all data for the transverse distribution of the chromoelectric field down to $x_t = 0$ is given in Fig. 1, where we also display the points calculated at noninteger distances, which were not included in the fit. We see that there are slight deviations from the fit curve due to the failure of rotational invariance on a discrete lattice. In fact, fitting all the available data to Eq. (8) results in an increase of the reduced chi-squared without affecting appreciably the fit parameters. In Table I, the results of our fit of Eq. (8) to the SU(2) data at $\beta = 2.52$ are reported. The Ginzburg-Landau parameter κ has been obtained through Eq. (10).

In Figs. 2–5 we display the fitted parameters versus the cooling steps. As regards the parameters μ, λ/ξ_v, and κ, a short plateau is always visible. This corroborates our expectation that the long-range physics is unaffected by the cooling procedure. On the other hand, Fig. 2 shows that the overall normalization of the transverse distribution of the longitudinal chromoelectric field is more affected by the cooling. In fact, the parameter ϕ seems to displays an approximate short plateau after 9–10 cooling steps, in accordance with previous studies [16].

TABLE I. Summary of the fit values for SU(2) at $\beta = 2.52$.

	SU(2) $\beta = 2.52$				
Cooling	ϕ	μ	λ/ξ_v	κ	χ^2_r
5	0.886(89)	0.829(267)	0.590(452)	0.512(400)	0.3
6	1.214(66)	0.782(145)	0.567(270)	0.485(365)	0.2
7	1.590(53)	0.749(82)	0.538(162)	0.453(325)	0.2
8	1.998(49)	0.711(51)	0.530(110)	0.444(314)	0.1
9	2.423(49)	0.685(39)	0.508(82)	0.420(285)	0.1
10	2.680(23)	0.652(22)	0.530(44)	0.444(313)	0.3

B. SU(3) data

We reanalyzed the SU(3) lattice data presented in Ref. [35]. We have fitted the longitudinal chromoelectric field transverse distribution to Eq. (8) for $\beta = 5.9$, 6.0, 6.05, 6.1 and up to 16 cooling steps. Again, we find that Eq. (8) accounts for the transverse distribution of the longitudinal chromoelectric field in the whole region

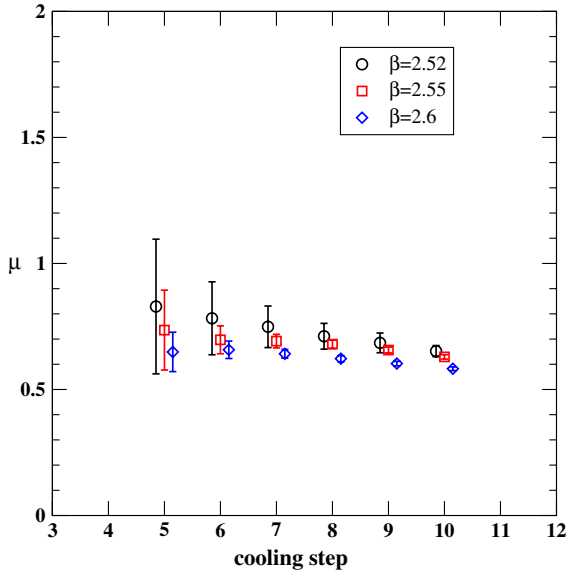

FIG. 3 (color online). SU(2): μ versus cooling. Here and in other figures below data have been slightly shifted along the horizontal axis for the sake of readability.

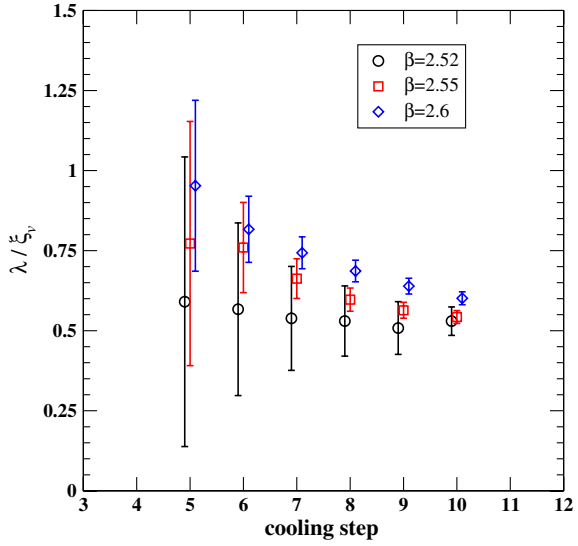

FIG. 4 (color online). SU(2): λ/ξ_v versus cooling.

$x_t \geq 0$. In Fig. 6, we display our data for the transverse shape of the longitudinal chromoelectric field between static quark-antiquark sources after 10 cooling steps at $\beta = 6.0$ together with the fit to Eq. (8). As for the SU(2) case, we also display the points calculated at noninteger distances and checked that the fit to all the available data of Eq. (8) does not change the values of the fit parameters.

In Table II, we collect the results of our fit of Eq. (8) to the SU(3) data at $\beta = 6.0$ for cooling steps ranging from 5 up to 16. In Figs. 7–10 we show the fitted parameters versus the cooling steps. In fact, we see that the parameters μ, λ/ξ_v, and κ, display a short plateau during the controlled cooling procedure as in the SU(2) case. Moreover, Fig. 7 shows that, at variance with the previous case, even the

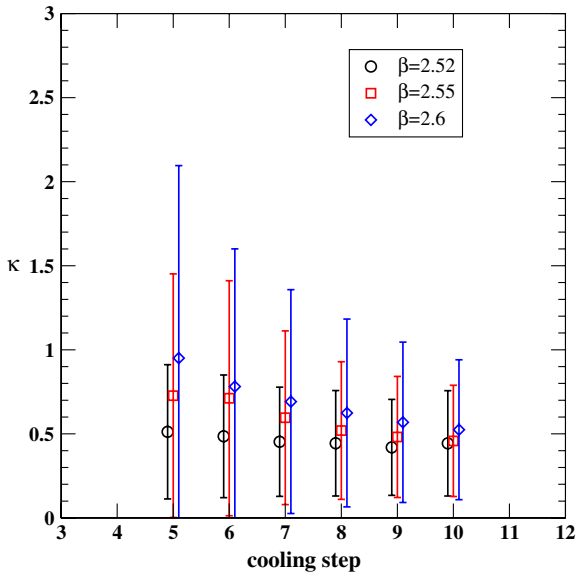

FIG. 5 (color online). SU(2): κ versus cooling.

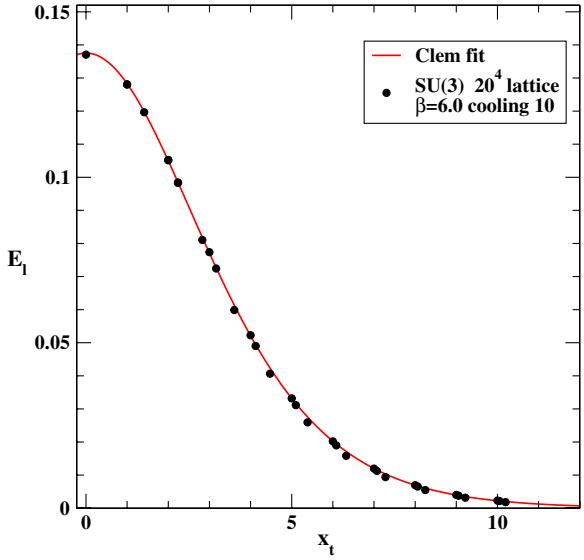

FIG. 6 (color online). SU(3): E_l at $\beta = 6.0$ after 10 cooling steps.

overall normalization of the transverse distribution of the longitudinal chromoelectric field ϕ seems to displays an approximate plateau after 7–9 cooling steps in agreement with the results of Ref. [35].

III. PENETRATION AND COHERENCE LENGTHS

In Refs. [16,35], it was found that the inverse penetration length μ exhibits approximate scaling with the string tension σ. To check the scaling of our new determination of μ with the string tension, we use a parametrization for the SU(2) string tension obtained by means of a Chebyshev polynomial interpolation to the string tension data collected in Table 10 of Ref. [50].

In Fig. 11, we display our determination of the ratio $\mu/\sqrt{\sigma}$ for three different values of β. For comparison we also report $\mu/\sqrt{\sigma}$, where the inverse of the penetration

TABLE II. Summary of the fit values for SU(3) at $\beta = 6.0$.

	SU(3) $\beta = 6.0$				
Cooling	ϕ	μ	λ/ξ_v	κ	χ^2_r
5	4.564(14)	0.726(8)	0.516(14)	0.428(295)	2.8
6	6.617(9)	0.683(4)	0.449(7)	0.355(216)	0.3
7	7.644(9)	0.652(4)	0.412(6)	0.316(177)	2.2
8	8.107(8)	0.630(3)	0.384(5)	0.287(150)	4.6
9	8.254(8)	0.612(3)	0.360(4)	0.263(130)	5.5
10	8.227(7)	0.598(3)	0.341(4)	0.244(114)	5.2
11	8.108(7)	0.585(3)	0.325(4)	0.229(103)	4.5
12	7.943(7)	0.574(3)	0.313(4)	0.217(94)	3.6
13	7.759(6)	0.563(3)	0.304(4)	0.208(88)	2.8
14	7.570(6)	0.553(3)	0.296(4)	0.201(83)	2.1
15	7.383(6)	0.544(3)	0.291(4)	0.196(79)	1.5
16	7.204(6)	0.534(3)	0.287(4)	0.192(77)	1.1

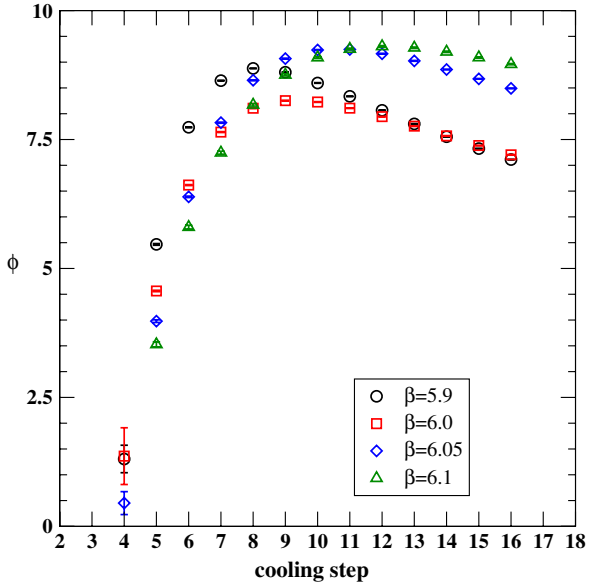

FIG. 7 (color online). SU(3): ϕ versus cooling.

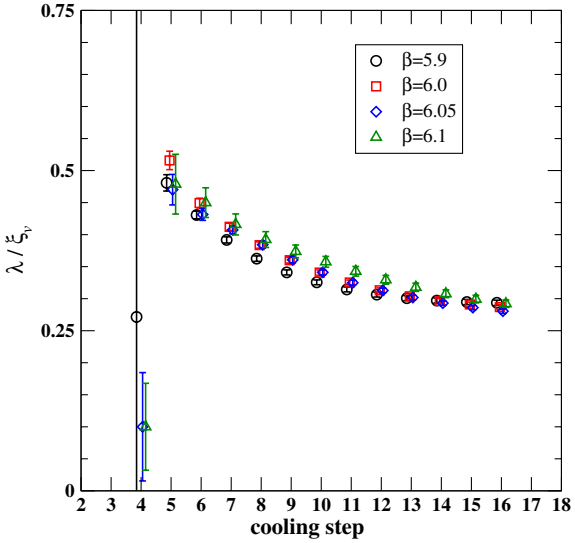

FIG. 9 (color online). SU(3): λ/ξ_v versus cooling.

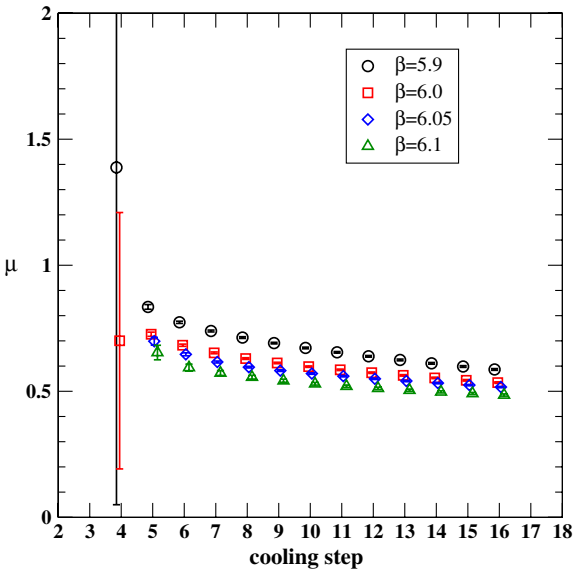

FIG. 8 (color online). SU(3): μ versus cooling.

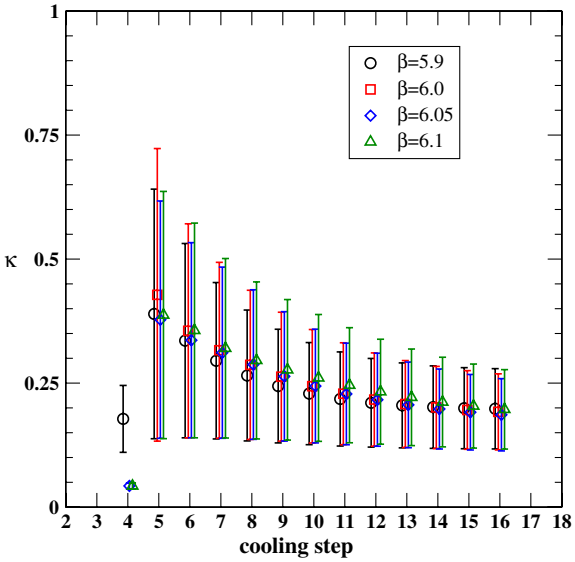

FIG. 10 (color online). SU(3): κ versus cooling.

length μ is obtained by fitting the transverse profile of the longitudinal chromoelectric field to Eq. (4) after eight cooling steps (for details, see Ref. [35]). We see that our new determination of $\mu/\sqrt{\sigma}$ is in satisfying agreement with the results of Ref. [35]. Thus, we confirm that μ displays an approximate scaling with the string tension σ. Fitting our data for $\mu/\sqrt{\sigma}$ with a constant, we estimate

$$\mu/\sqrt{\sigma} = 4.133(98), \tag{11}$$

where the quoted error takes care also of the systematic errors due to the scaling violations displayed by our data.

Assuming $\sqrt{\sigma} = 420$ MeV, Eq. (11) gives for the penetration length

$$\lambda = \frac{1}{\mu} = 0.1135(27) \text{ fm}. \tag{12}$$

Moreover, we have also checked the scaling of the Ginzburg-Landau parameter κ obtained through Eq. (10). In fact, Fig. 12 shows that κ is almost insensitive to β. By fitting the data with a constant we get

$$\kappa = 0.467 \pm 0.310. \tag{13}$$

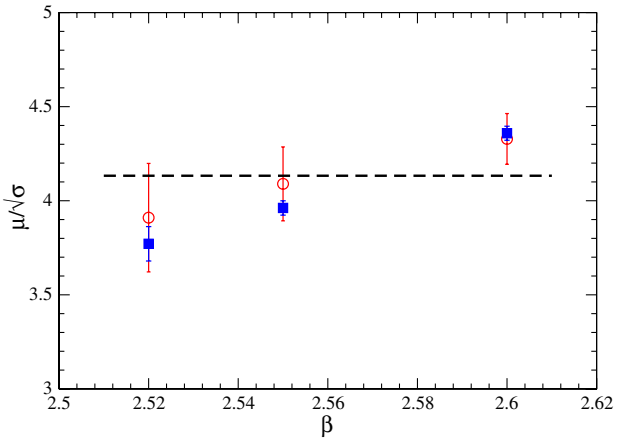

FIG. 11 (color online). SU(2): $\mu/\sqrt{\sigma}$ versus β. Open circles corresponds to the fit with Eq. (4) after eight cooling steps, full squares correspond to the fit with Eq. (8) after 10 cooling steps.

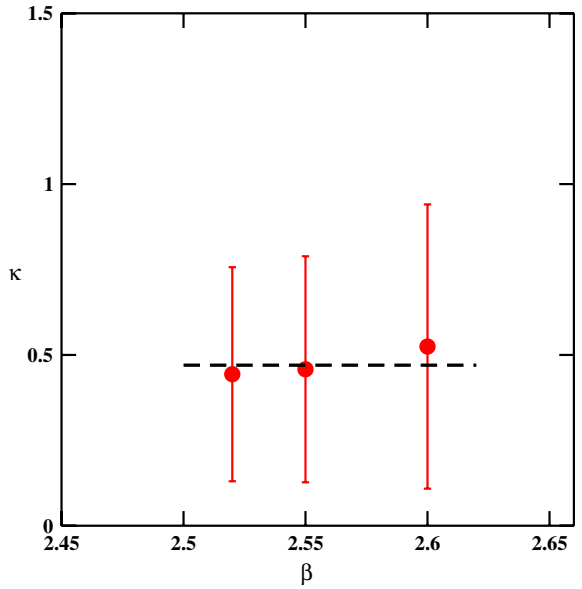

FIG. 12 (color online). SU(2): κ versus β for 10 cooling steps.

We would like to stress that our continuum extrapolation for the penetration length and the Ginzburg-Landau parameter are in reasonable agreement with the results obtained in Refs. [43,44,51]. In particular, we may confirm that the Ginzburg-Landau parameter is consistent with the critical value $\kappa_c = \frac{1}{\sqrt{2}}$, i.e., the SU(2) vacuum behaves as a dual superconductor which lies at the borderline between the type I-type II superconductor regions.

Also, for the SU(3) gauge theory, we studied the scaling of the "plateau" values of μ with the string tension. For this purpose, we have expressed our values of μ in units of $\sqrt{\sigma}$, using the parametrization

$$\sqrt{\sigma}(g) = f_{\mathrm{SU(3)}}(g^2)[1 + 0.2731\hat{a}^2(g) - 0.01545\hat{a}^4(g) + 0.01975\hat{a}^6(g)]/0.01364, \quad (14)$$

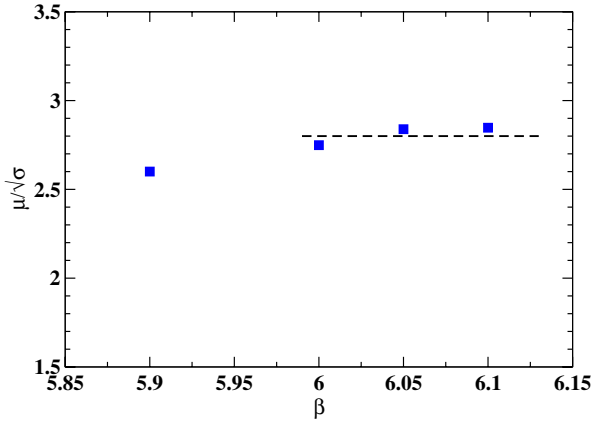

FIG. 13 (color online). SU(3): $\mu/\sqrt{\sigma}$ versus β. Full squares correspond to the fit with Eq. (8) after 10 cooling steps.

$$\hat{a}(g) = \frac{f_{\mathrm{SU(3)}}(g^2)}{f_{\mathrm{SU(3)}}(g^2(\beta = 6))}, \qquad \beta = \frac{6}{g^2}, \qquad 5.6 \le \beta \le 6.5,$$
$$f_{\mathrm{SU(3)}}(g^2) = (b_0 g^2)^{-b_1/2b_0^2} \exp\left(-\frac{1}{2b_0 g^2}\right),$$
$$b_0 = \frac{11}{(4\pi)^2}, \qquad b_1 = \frac{102}{(4\pi)^4}, \quad (15)$$

given in Ref. [52]. Figure 13 suggests that the ratio $\mu/\sqrt{\sigma}$ displays a nice plateau in β, as soon as β is larger than 6. Accordingly, fitting the ratio $\mu/\sqrt{\sigma}$ to a constant we get:

$$\frac{\mu}{\sqrt{\sigma}} = 2.799(38), \quad (16)$$

which, assuming again the standard value for the string tension $\sqrt{\sigma} = 420$ MeV, corresponds to:

$$\lambda = \frac{1}{\mu} = 0.1676(23) \text{ fm}. \quad (17)$$

The quoted error takes into account our estimation of systematic effects due to the small scaling violations present in our lattice data. It is interesting to compare the present determination of the SU(3) penetration length with the one obtained previously [35] by fitting the lattice data to Eq. (4). In fact in Ref. [35] we obtained $\frac{\mu}{\sqrt{\sigma}} = 2.325(5)$ which, unlike the SU(2) gauge theory, seems not to agree with Eq. (16). This discrepancy must be ascribed to the fact that, as discussed below, in the present case the coherence length exceeds the penetration length. In other words, the SU(3) vacuum behaves like a type I superconductor and, as we already discussed, the London equation Eq. (4) is not good enough to describe the transverse distribution of the longitudinal chromoelectric field.

As concerns the Ginzburg-Landau parameter, in Fig. 14 we present our lattice data for different values of β. Indeed, κ is almost insensitive to β. By fitting the data with a constant we get

$$\kappa = 0.243 \pm 0.088, \quad (18)$$

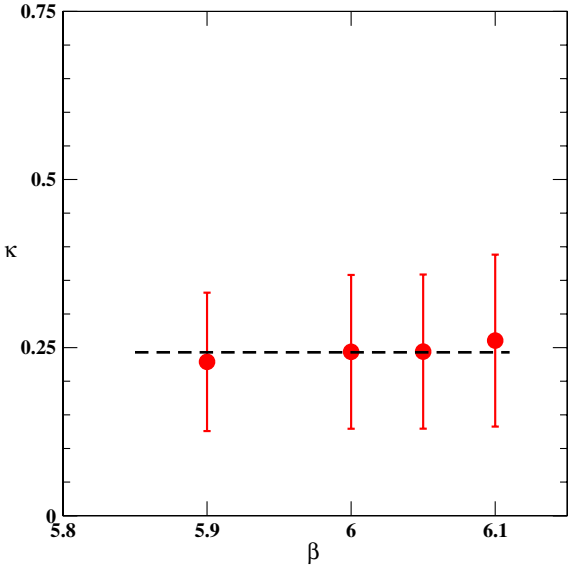

FIG. 14 (color online). SU(3): κ versus β for 10 cooling steps.

which confirms that $\kappa < \kappa_c$ (type I superconductor). It is worthwhile to note that our Eqs. (17) and (18) are not in agreement with the recent determinations in Ref. [53], where it is reported $\lambda = 0.2013(174)$ fm and $\kappa = 1.218(109)$. We believe that the origin of the discrepancies resides in the use of different lattice operators to extract the longitudinal chromoelectric field. In fact, the authors of Ref. [53] use a lattice operator which is sensitive to the square of the chromoelectric field instead of our correlation function, Eq. (1), which measures the chromoelectric field strength. In any case, we believe that these discrepancies deserve further studies. To summarize, we have found that the transverse behavior of the longitudinal chromoelectric field can be fitted according to Eq. (6) for both SU(2) and SU(3) gauge theories. This allows us to determine the coherence and penetration lengths. In Ref. [35], it was stressed that the ratio between the penetration lengths respectively for SU(2) and SU(3) gauge theories recalls the analogous behavior seen in a different study of SU(2) and SU(3) vacuum in a constant external chromomagnetic background field [54]. In fact, in Ref. [54] numerical evidence was presented that the deconfinement temperature for SU(2) and SU(3) gauge systems in a constant Abelian chromomagnetic field decreases when the strength of the applied field increases. Moreover, as discussed in Refs. [26,54,55], above a critical strength $\sqrt{gH_c}$ of the chromomagnetic external background field the deconfined phase extends to very low temperatures. It was found [54] that the ratio between the critical field strengths for SU(2) and SU(3) gauge theories was

$$\frac{\sqrt{gH_c}|_{\mathrm{SU(2)}}}{\sqrt{gH_c}|_{\mathrm{SU(3)}}} = 2.03(17). \tag{19}$$

It is interesting to compare the ratio between the critical field strengths Eq. (19) with the analogous ratio between penetration and coherence lengths. Combining Eqs. (5), (11), (13), (16), and (18), we readily obtain

$$\frac{\lambda_{\mathrm{SU(3)}}}{\lambda_{\mathrm{SU(2)}}} = \frac{\mu_{\mathrm{SU(2)}}}{\mu_{\mathrm{SU(3)}}} = 1.48(4), \tag{20}$$

$$\frac{\xi_{\mathrm{SU(3)}}}{\xi_{\mathrm{SU(2)}}} = 2.84 \pm 2.15. \tag{21}$$

It is remarkable that the ratio between the penetration lengths, respectively for SU(3) and SU(2) gauge theories, agrees with the analogous ratio between the coherence lengths, albeit within the rather large statistical uncertainty. Moreover, both ratios are in fair agreement with the ratio between the critical field strengths, Eq. (19).

As stressed in the conclusions of Ref. [54], the peculiar dependence of the deconfinement temperature on the strength of the Abelian chromomagnetic field gH could be naturally explained if the vacuum behaved as a disordered chromomagnetic condensate which confines color charges due both to the presence of a mass gap and the absence of color long-range order, such as in the Feynman picture for Yang-Mills theory in $(2 + 1)$ dimensions [56]. The circumstance that the ratio between the SU(2) and SU(3) penetration and coherence lengths agrees within errors with the above discussed ratio of the critical chromomagnetic fields, suggests us that the Feynman picture of the Yang-Mills vacuum could be a useful guide to understand the dynamics of color confinement.

IV. CHROMOELECTRIC FLUX TUBE AND STRING TENSION

We have shown [16,35] that the color fields of a static quark-antiquark pair are almost completely described by the longitudinal chromoelectric field, which in turn is approximately constant along the flux tube. This means that the long-distance potential acting on the color charges is linear. Using our data and the parametrization Eq. (8) for the chromoelectric flux tube, we are able to compute the string tension given as the energy stored into the flux tube per unit length

$$\sigma_{E_l} \simeq \frac{1}{2} \int d^2x_t E_l^2(x_t), \tag{22}$$

where, to avoid confusion, we have denoted the flux-tube string tension as σ_{E_l}, while σ will indicate the lattice string tension. It is worth noting that the string tension σ_{E_l} defined by Eq. (22) does not depend on x_l as long as the longitudinal chromoelectric field is constant along the flux tube. Obviously this last condition is not strictly fulfilled on a finite lattice. From Eqs. (8) and (22) we obtain an explicit relation between the string tension and the parameters ϕ, μ, and α of the fit Eq. (8) to the chromoelectric flux tube profile

$$\sigma_{E_l} = \frac{1}{4\pi}\frac{\phi^2\mu^4}{\alpha^2}\frac{1}{K_1^2(\alpha)}\int_0^\infty dr r K_0^2((\mu^2 r^2+\alpha^2)^{1/2}). \quad (23)$$

After performing the integration, we get

$$\frac{\sqrt{\sigma_{E_l}}}{\mu} = \left(\frac{\phi^2}{8\pi}\left(1-\frac{K_0^2(\alpha)}{K_1^2(\alpha)}\right)\right)^{1/2}. \quad (24)$$

Naively, one expects that the string tension defined as the energy per unit length stored into the flux tube chromoelectric field Eq. (24) should agree, at least approximatively, with the string tension measured on the lattice. To check this, in Figs. 15 and 16 we compare the flux-tube string tension in Eq. (24) with the lattice string tension (obtained as detailed in the previous section) for SU(2) and SU(3) gauge theories, respectively. It is evident from Figs. 15 and 16 that

$$\sigma_{E_l} > \sigma, \quad (25)$$

for both SU(2) and SU(3) gauge theories. At first sight this result looks quite surprising. In fact, the lattice string tension should contain the total energy per unit length stored into the flux tube. As a consequence we can write

$$\sigma \simeq \sigma_{E_l} + \sigma_{\rm cond}, \quad (26)$$

where $\sigma_{\rm cond}$ takes into account the contribution due to the order parameter condensate. We may, in turn, obtain an estimate of this contribution to the total string tension as follows. Since within the vortex core the order parameter condensate vanishes, we have

$$\sigma_{\rm cond} \simeq -\pi\xi^2\varepsilon_{\rm cond}, \quad (27)$$

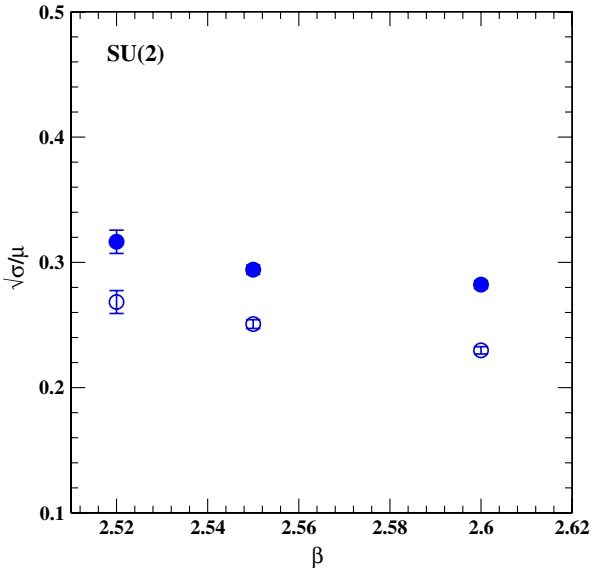

FIG. 15 (color online). SU(2): $\sqrt{\sigma}/\mu$ versus β. Full points correspond to Eq. (24); open points refer to the lattice string tension (see the discussion in the text).

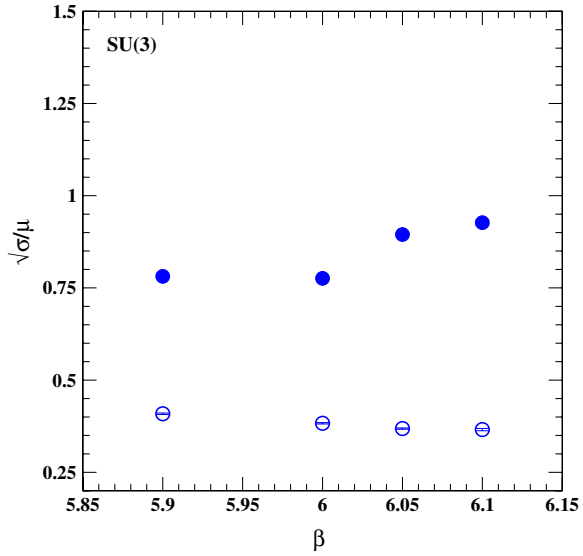

FIG. 16 (color online). SU(3): $\sqrt{\sigma}/\mu$ versus β. Full points correspond to Eq. (24); open points refer to the lattice string tension (see the discussion in the text).

where $\varepsilon_{\rm cond}$ is the condensation energy density and ξ is approximately the vortex core size. Note that the minus sign is due to the loss of condensation energy in the normal region with respect to the confining vacuum, where the order parameter is nonzero. Now, it is usually assumed that in the confining vacuum it is energetically favored to have a condensation of the order parameter as in ordinary BCS superconductors, where the superconducting transition is energetically driven by the coherent condensation of Cooper pairs. Therefore, one is led naturally to suppose that $\varepsilon_{\rm cond} < 0$. Thus we see from Eqs. (26) and (27) that one should obtain $\sigma_{E_l} < \sigma$. On the contrary, our numerical results clearly indicate that σ_{E_l} exceeds σ. The only possible conclusion we can derive is that the order parameter condensation energy is positive. Thus, the confining transition must be driven by disordering the gauge system. In other words, even though the condensation of the confining order parameter costs energy there is a huge number of degenerate physical configurations such that the configurational entropy easily overcomes the energy cost. This means that the deconfining transition is an order-disorder transition, much more like the Berezinskii-Kosterlitz-Thouless transition than the BCS superconducting transition. It is remarkable that this conclusion reinforces our previous picture of the confining vacuum that behaves like a disordered chromomagnetic condensate which confines color charges due both to the presence of a mass gap and the absence of color long-range order, such as in the Feynman qualitative picture [56].

V. CONCLUSIONS

In the present paper we studied the chromoelectric field distribution between a static quark-antiquark pair in

SU(2) and SU(3) pure gauge theories. By means of the connected correlator given in Eq. (1) we were able to compute the chromoelectric field that fills the flux tube along the line joining a quark-antiquark pair. Since our connected correlator is sensitive to the field strengths instead of the squared field strength, we were able to follow the transverse shape of the color fields up to sizable distances. Using some dated results in ordinary superconductivity based on a simple variational model for the magnitude of the normalized order parameter of an isolated vortex, we proposed that the transverse behavior of the longitudinal chromoelectric field can be fitted according to Eq. (8), which allowed us to get informations on the penetration and coherence lengths. In fact we found that our Eq. (8) is able to reproduce the transverse distribution of the longitudinal chromoelectric field in the whole available region. In the case of the SU(2) gauge theory we argued that the confining vacuum behaves as a dual superconductor that lies at the borderline between the superconductor type I and type II regions. On the other hand, we found that the SU(3) vacuum belongs to the superconductor type I region. We found that the ratio between the penetration lengths respectively for SU(3) and SU(2) gauge theories agrees with the analogous ratio between the coherence lengths, albeit within the rather large statistical uncertainty, and both ratios are in fair agreement with the ratio between the critical chromomagnetic fields. Finally, we suggested that the deconfining transition resembles the order-disorder Berezinskii-Kosterlitz-Thouless transition and that the confining vacuum behaves like a disordered chromomagnetic condensate in agreement with the Feynman qualitative picture of the Yang-Mills vacuum.

[1] M. Bander, Phys. Rep. **75**, 205 (1981).
[2] J. Greensite, Prog. Part. Nucl. Phys. **51**, 1 (2003).
[3] M. Fukugita and T. Niuya, Phys. Lett. **132B**, 374 (1983).
[4] J. E. Kiskis and K. Sparks, Phys. Rev. D **30**, 1326 (1984).
[5] J. W. Flower and S. W. Otto, Phys. Lett. **160B**, 128 (1985).
[6] J. Wosiek and R. W. Haymaker, Phys. Rev. D **36**, 3297 (1987).
[7] A. Di Giacomo, M. Maggiore, and S. Olejnik, Phys. Lett. B **236**, 199 (1990).
[8] A. Di Giacomo, M. Maggiore, and S. Olejnik, Nucl. Phys. **B347**, 441 (1990).
[9] V. Singh, D. A. Browne, and R. W. Haymaker, Phys. Lett. B **306**, 115 (1993).
[10] P. Cea and L. Cosmai, Nucl. Phys. B, Proc. Suppl. **30**, 572 (1993).
[11] Y. Matsubara, S. Ejiri, and T. Suzuki, Nucl. Phys. B, Proc. Suppl. **34**, 176 (1994).
[12] P. Cea and L. Cosmai, Nuovo Cimento Soc. Ital. Fis. **107A**, 541 (1994).
[13] P. Cea and L. Cosmai, Nucl. Phys. B, Proc. Suppl. **34**, 219 (1994).
[14] P. Cea and L. Cosmai, Phys. Lett. B **349**, 343 (1995).
[15] P. Cea and L. Cosmai, Nucl. Phys. B, Proc. Suppl. **42**, 225 (1995).
[16] P. Cea and L. Cosmai, Phys. Rev. D **52**, 5152 (1995).
[17] G. S. Bali, K. Schilling, and C. Schlichter, Phys. Rev. D **51**, 5165 (1995).
[18] R. W. Haymaker and T. Matsuki, Phys. Rev. D **75**, 014501 (2007).
[19] A. D'Alessandro, M. D'Elia, and L. Tagliacozzo, Nucl. Phys. **B774**, 168 (2007).
[20] G. 't Hooft, in *High Energy Physics, EPS International Conference, Palermo, 1975*, edited by A. Zichichi (Editrice Compositori, Bologna, 1976).
[21] S. Mandelstam, Phys. Rep. **23**, 245 (1976).
[22] G. Ripka, Lect. Notes Phys. **639**, 1 (2004).
[23] H. Shiba and T. Suzuki, Phys. Lett. B **351**, 519 (1995).
[24] N. Arasaki, S. Ejiri, S.-i. Kitahara, Y. Matsubara, and T. Suzuki, Phys. Lett. B **395**, 275 (1997).
[25] P. Cea and L. Cosmai, Phys. Rev. D **62**, 094510 (2000).
[26] P. Cea and L. Cosmai, J. High Energy Phys. 11 (2001) 064.
[27] A. Di Giacomo, B. Lucini, L. Montesi, and G. Paffuti, Phys. Rev. D **61**, 034503 (2000).
[28] A. Di Giacomo, B. Lucini, L. Montesi, and G. Paffuti, Phys. Rev. D **61**, 034504 (2000).
[29] J. M. Carmona, M. D'Elia, A. Di Giacomo, B. Lucini, and G. Paffuti, Phys. Rev. D **64**, 114507 (2001).
[30] P. Cea, L. Cosmai, and M. D'Elia, J. High Energy Phys. 02 (2004) 018.
[31] A. D'Alessandro, M. D'Elia, and E. V. Shuryak, Phys. Rev. D **81**, 094501 (2010).
[32] G. 't Hooft, in *Large NC QCD 2004, Proceedings of the Workshop at Trento, Italy, 5-11 July 2004*, edited by J. L. Goity, R. F. Lebed, A. Pich, C. L. Schat, and N. N. Scoccola (World Scientific, Singapore, 2005).
[33] A. A. Abrikosov, Zh. Eksp. Teor. Fiz. **32**, 1442 (1957) [Sov. Phys. JETP **5**, 1174 (1957)].
[34] H. B. Nielsen and P. Olesen, Nucl. Phys. **B61**, 45 (1973).
[35] M. S. Cardaci, P. Cea, L. Cosmai, R. Falcone, and A. Papa, Phys. Rev. D **83**, 014502 (2011).
[36] J. R. Clem, J. Low Temp. Phys. **18**, 427 (1975).
[37] D. S. Kuzmenko and Y. A. Simonov, Phys. Lett. B **494**, 81 (2000).
[38] A. Di Giacomo, H. G. Dosch, V. I. Shevchenko, and Y. A. Simonov, Phys. Rep. **372**, 319 (2002).
[39] T. Suzuki, Prog. Theor. Phys. **80**, 929 (1988).
[40] S. Maedan, Y. Matsubara, and T. Suzuki, Prog. Theor. Phys. **84**, 130 (1990).
[41] V. Singh, D. A. Browne, and R. W. Haymaker, Nucl. Phys. B, Proc. Suppl. **30**, 568 (1993).

[42] Y. Matsubara, S. Ejiri, and T. Suzuki, Nucl. Phys. B, Proc. Suppl. **34**, 176 (1994).
[43] C. Schlichter, G. S. Bali, and K. Schilling, Nucl. Phys. B, Proc. Suppl. **63**, 519 (1998).
[44] G. S. Bali, C. Schlichter, and K. Schilling, Prog. Theor. Phys. Suppl. **131**, 645 (1998).
[45] K. Schilling, G. Bali, and C. Schlichter, Nucl. Phys. B, Proc. Suppl. **73**, 638 (1999).
[46] F. Gubarev, E.-M. Ilgenfritz, M. Polikarpov, and T. Suzuki, Phys. Lett. B **468**, 134 (1999).
[47] Y. Koma, E.-M. Ilgenfritz, H. Toki, and T. Suzuki, Phys. Rev. D **64**, 011501 (2001).
[48] Y. Koma, M. Koma, E.-M. Ilgenfritz, and T. Suzuki, Phys. Rev. D **68**, 114504 (2003).
[49] M. Campostrini, A. Di Giacomo, M. Maggiore, H. Panagopoulos, and E. Vicari, Phys. Lett. B **225**, 403 (1989).
[50] M. J. Teper, arXiv:hep-th/9812187.
[51] T. Suzuki, K. Ishiguro, Y. Koma, and T. Sekido, Phys. Rev. D **77**, 034502 (2008).
[52] R. G. Edwards, U. M. Heller, and T. R. Klassen, Nucl. Phys. **B517**, 377 (1998).
[53] N. Cardoso, M. Cardoso, and P. Bicudo, arXiv:1004.0166.
[54] P. Cea and L. Cosmai, J. High Energy Phys. 08 (2005) 079.
[55] P. Cea, L. Cosmai, and M. D'Elia, J. High Energy Phys. 12 (2007) 097.
[56] R. P. Feynman, Nucl. Phys. **B188**, 479 (1981).